JOURNAL OF
Materials
CHEMISTRY

Thermo-Raman investigations on structural transformations in hydrated MoO_3

Ramaswamy Murugan,† Anil Ghule, Chetan Bhongale and Hua Chang*

Department of Chemistry, National Tsing Hua University, Hsinchu, Taiwan, 30034, Republic of China

Received 31st January 2000, Accepted 14th June 2000
Published on the Web 25th July 2000

Thermally induced structural transformations in hydrated MoO_3 prepared by acidification of Na_2MoO_4 solution have been investigated dynamically by thermo-Raman spectroscopic techniques. The thermo-Raman spectra reveal that the structural evolution of as-synthesized hydrated MoO_3 in air proceeds through an amorphous phase after dehydration processes, formation of sub-microcrystals, the MoO_3-II phase (possible) and the α-MoO_3 phase in a dynamic thermal process. The thermo-Raman results are supported by thermogravimetry, differential thermal analysis, differential scanning calorimetry and powder X-ray diffraction results. The structural evolution of as-synthesized hydrated MoO_3 under nitrogen gas flow was also investigated by thermo-Raman studies.

Introduction

Molybdenum trioxide (MoO_3) is a versatile transition-metal oxide material and finds important applications in diverse areas. MoO_3 is known to exist in a variety of oxides, sub-oxides, hydroxides and crystalline hydrates.[1] The MoO_3 hydrates include monoclinic dihydrate ($MoO_3 \cdot 2H_2O$), two forms of monohydrates ($MoO_3 \cdot H_2O$; yellow monoclinic monohydrate and white triclinic monohydrate), monoclinic hemihydrate ($MoO_3 \cdot 1/2H_2O$) and orthorhombic $MoO_3 \cdot 1/3H_2O$.[2] Three different crystalline polymorphs of MoO_3, stable orthorhombic α-MoO_3, metastable β-MoO_3 and the metastable high-pressure phase MoO_3-II, have been reported.[3–5]

Haro-Poniatowski *et al.* recently reported the preparation of hydrated MoO_3 by acidification of sodium molybdate (Na_2MoO_4) solution and also revealed the dependence of the morphology and color of the resulting product on the drying procedure.[6] Using Raman scattering techniques, they demonstrated the evolution of the sample from a low temperature glass phase to a high temperature glass phase then crystallization under laser irradiation. Although studies on dehydration and phase transformations in hydrated MoO_3 by TG (thermogravimetry),[3,4,7] DTA (differential thermal analysis),[8] DSC (differential scanning calorimetry)[4] and XRD (X-ray diffraction)[3] are extensive, there are still several inconsistencies regarding the number of dehydration steps and the nature of the phase transformations. However, dynamic studies on the structural evolution of hydrated MoO_3 as a function of temperature are scarce.

Raman spectroscopy is one of the most convenient and powerful tools to unravel details about local and cooperative changes during transformations between phases. Raman spectra can be measured dynamically as a function of temperature during a thermal process, a technique known as thermo-Raman spectroscopy. This can provide valuable information for the *in situ* investigation of composition changes and phase transformations.[9–14] In this work, the dynamics involved in the dehydration processes, transformations from amorphous phase to crystalline phase and transformations between crystalline polymorphs of MoO_3 were studied extensively by thermo-Raman spectroscopy in air in a dynamic thermal process. The results were supported by thermal analysis, TG, DTA and DSC. A systematic PXRD (powder X-ray diffraction) investigation of the samples after heat treatment to various temperatures was carried out to probe the structural evolution. The dynamic thermal evolution of as-synthesized hydrated MoO_3 under a nitrogen atmosphere was also investigated by thermo-Raman studies.

Experimental

The hydrated MoO_3 used in this work was prepared by passing an acidic aqueous solution of Na_2MoO_4 (1 mol L^{-1}) through proton exchange resin. A light blue molybdic acid solution was obtained and was partially dried under vacuum at room temperature. The solid obtained was light blue in colour.

Raman scattering was excited with an argon ion laser (Coherent, Innova 100-15) operating at a wavelength of 514.5 nm. The scattered radiation was collected, analyzed by a 0.5 m spectrophotometer (Spex) and detected by a CCD camera (Princeton Instruments, 1024 × 1024 pixels). Spectra were taken continuously with a 12 s exposure time, such that each spectrum covered 1 °C in a dynamic thermal process, heating from 25 to 500 °C at a rate of 5 °C min^{-1} in air or under a nitrogen atmosphere. A low laser power of 10 mW was employed for the thermo-Raman studies to avoid any heating effect due to laser irradiation. The spectral resolution was about 2 cm^{-1}.

The DSC (Seiko I DSC-200) thermogram was measured in a flow of air from 25 to 500 °C at a heating rate of 5 °C min^{-1}. TG and DTA (Seiko I SSC 5000 TGA/DTA) thermograms were also recorded in the same thermal process.

PXRD analyses were performed on the as-synthesized hydrated MoO_3 sample and samples after heat treatment to 125, 255, 310, 350, 420 and 500 °C at a heating rate of 5 °C min^{-1} in air to study the crystallization process. The PXRD (Shimadzu XD-5 diffractometer) patterns were recorded using Cu-Kα radiation at a scan rate of 4° (2θ) min^{-1}.

Results and discussion

The TG thermogram and its derivative DTG thermogram measured from 25 to 500 °C at a heating rate of 5 °C min^{-1} for the as-synthesized hydrated MoO_3 sample are shown in

---

†On leave from Department of Physics, Pondicherry Engineering College, Pondicherry, 605 014, India.

DOI: 10.1039/b000811g

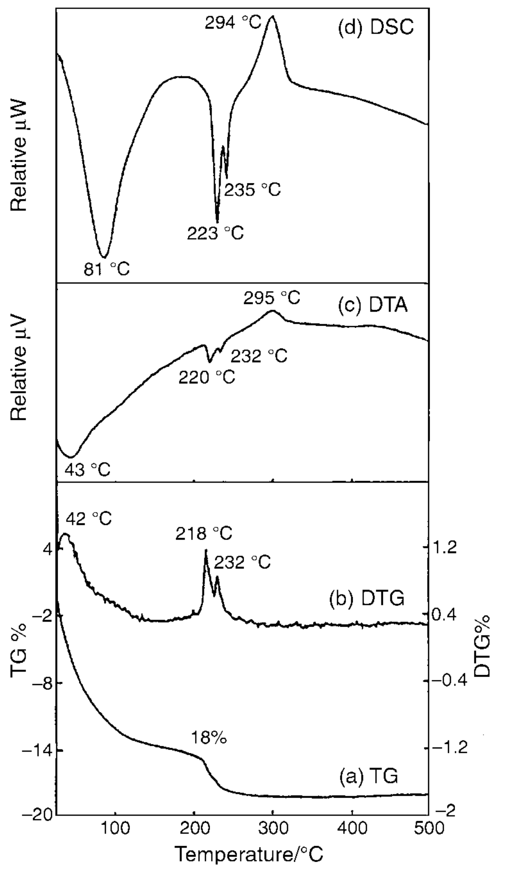

Fig. 1 (a) TG, (b) DTG, (c) DTA and (d) DSC thermograms of as-synthesized hydrated MoO_3 measured from 25 to 500 °C at a heating rate of 5 °C min^{-1}.

Fig. 1(a) and 1(b), respectively. Both thermograms show a major weight loss in the range 25 to 120 °C, with a maximum around 42 °C, corresponding to the dehydration process. They also show two minor weight losses around 218 and 232 °C. The total weight loss was about 18%, which was 2% less than the calculated value for $MoO_3{\cdot}2H_2O$. DTA and DSC thermograms measured under similar experimental conditions are shown in Fig. 1(c) and 1(d), respectively. The DTA thermogram shows endotherms at 43, 220 and 232 °C, corresponding to the three weight losses observed in the TG, and a broad exotherm around 295 °C. There is a deviation in the baseline around 400 °C and a continuous decrease in the baseline at higher temperatures. The DSC thermogram also shows endotherms at 81, 223 and 235 °C, corresponding to the three weight losses observed in TG. Similar to the DTA thermogram, the DSC thermogram shows a broad exotherm at 294 °C, a deviation in the baseline around 390 °C and a continuous decrease in the baseline at higher temperatures. The three weight losses observed in the TG and their corresponding endotherms in the DTA and DSC might be due to dehydration processes. As the crystallization takes place, the heat of crystallization is evolved and an exothermic peak appears on the DTA and DSC thermograms around 295 °C, as shown in Fig. 1(c) and 1(d). The observation of a slight deviation in the baseline around 390 °C in both the DTA and DSC thermograms might be due to transformation between polymorphic phases of MoO_3.

A set of thermo-Raman spectra were collected as a function of temperature during a dynamic thermal process from 25 to 500 °C at a heating rate of 5 °C min^{-1} in air for the *in situ* investigation of composition changes and phase transformations. Water vibrations in hydrated MoO_3 have been discussed earlier by Seguin *et al.*[2] The water content in the hydrated MoO_3 prepared by acidification of Na_2MoO_4 solution depends upon the drying procedures. The Raman spectra of water in hydrated crystals usually show extremely broad bands, making interpretation difficult. Particularly, the in plane bending vibrations of water are too weak to be observed in Raman spectra. Also the librational modes of water, which usually appear with low intensity in the low frequency region, overlap with other modes and are difficult to identify.

Fig. 2 represents the spectral variations observed in the water vibration region from 40 to 120 °C. The spectrum observed at 40 °C shows a profile composed of a very broad band with a maximum at 3470 cm^{-1} and a weak broad shoulder centered around 3185 cm^{-1}, corresponding to typical stretching vibrations of hydrated water molecules. Spectral variations, shown in Fig. 2, clearly show that the major intensity loss of the broad band at 3470 cm^{-1} and the disappearance of the weak band at 3185 cm^{-1} from 60 to 80 °C correspond to the main dehydration process. The spectrum observed at 90 °C shows a very weak band at 3470 cm^{-1} which loses its intensity with further increases in temperature and almost vanishes around 120 °C. Since water is a weak scatterer, it proved very difficult to ascertain by thermo-Raman spectroscopy whether the two small weight losses observed around 218 and 231 °C in the TG and the corresponding endotherms in the DTA and DSC were associated with the minor dehydration processes.

The Mo–O stretching and bending vibrations in hydrated MoO_3 samples usually appear around the 1000–600 and 600–400 cm^{-1} regions, respectively.[15] The spectral variations observed from 30 to 120 °C, shown in Fig. 3, clearly show the effect of the major dehydration process in the Mo–O vibration region. The Raman spectrum of as-synthesized hydrated MoO_3 at 30 °C shows a strong sharp band at 948 cm^{-1} and another strong but broad band around 877 cm^{-1}. Additionally, two broad bands centered around 694 and 230 cm^{-1} and weak bands at 563, 515, 456 and 372 cm^{-1} are also observed. In addition to the broadening of all the bands, the overall intensity of the entire spectrum is reduced drastically from 50 °C. The intensity of the band at 877 cm^{-1} is less than that of the band at 948 cm^{-1} in the 30 to 50 °C interval but then becomes greater. The spectrum measured around 120 °C shows two broad structureless features at 954 and 859 cm^{-1} for the amorphous phase.

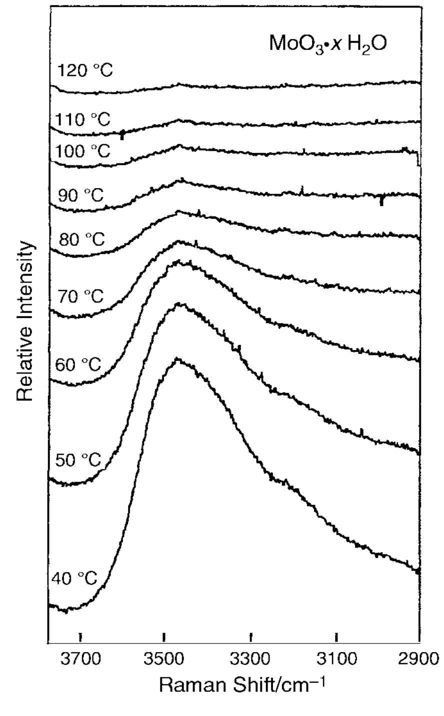

Fig. 2 Thermo-Raman spectra of as-synthesized hydrated MoO_3 in the vibration region of water from 40 to 120 °C.

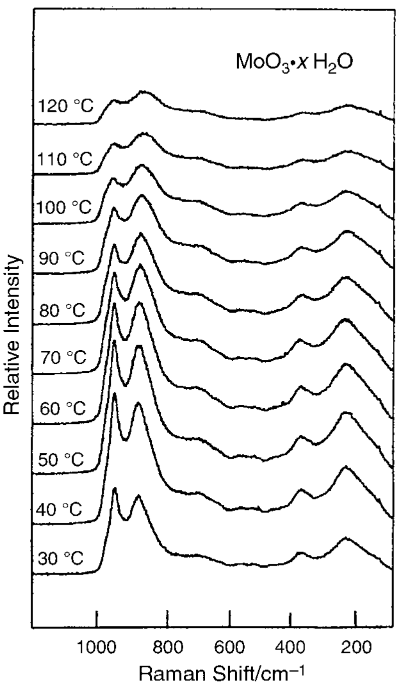

Fig. 3 Thermo-Raman spectra of as-synthesized hydrated MoO_3 in the vibration region of MoO_3 from 30 to 120 °C during dehydration.

Apparently, Fig. 3 shows the variation of the Raman spectrum in the Mo–O vibration region during the major dehydration process.

The spectral variations observed in the temperature interval 160 to 250 °C, shown in Fig. 4, indicate the effect of two small weight losses around 200 and 230 °C, due to two minor dehydration processes, on the thermo-Raman spectra and also reveal the amorphous nature of the sample in this temperature range. The spectrum recorded at 220 °C differs from the spectrum at 160 °C in that the two broad bands and other remaining weak bands disappear but a weak band at 815 cm^{-1} develops on a plateau from 200 °C. Apart from the weak band at 815 cm^{-1}, the spectrum shows no features. This confirms the amorphous nature of the sample at this temperature. Similarly, around 230 °C, in addition to the band at 815 cm^{-1}, another weak band at 990 cm^{-1} appears. The spectrum recorded at 250 °C clearly shows that the increase in intensity of the bands at 815 and 990 cm^{-1} and the appearance of a few very weak bands at lower frequencies signals the formation of sub-microcrystals.

The spectral variation observed in the temperature interval 280 to 325 °C, shown in Fig. 5, clearly reveals the growth in the size of microcrystals in the crystallization growth process with increasing temperature. The increase in intensity of all bands, due to an increase in concentration of crystalline phase, and decrease in line width of the dominant modes, due to an increase in the correlation length of the vibrations, are consistent with the growth of sub-microcrystals.

The spectra observed in the temperature interval 350 to 440 °C, shown in Fig. 6, reveal no major change in the spectral profile but an appreciable increase in the intensities of the bands from 400 °C. Baker *et al.* reported that the topotactic dehydration of either white $MoO_3 \cdot H_2O$ or $MoO_3 \cdot 1/2H_2O$ leads to a metastable high pressure MoO_3-II phase at ambient conditions and conversion of the MoO_3-II phase to α-MoO_3 phase at high temperature.[5] They also reported that the conversion of the MoO_3-II phase to α-MoO_3 phase involved a change in the stacking sequence of $MoO_{1/1}O_{2/2}O_{3/3}$ layers, from aaa (mono) to aba (ortho). The individual layer remains unchanged, hence the Raman spectra of the MoO_3-II and α-MoO_3 phases are similar, except for some slight variations in the low frequency region. The Raman spectrum observed in this work at 320 °C (Fig. 5) was more similar to the spectrum of the MoO_3-II phase provided by Baker *et al.*[5] In the temperature range 250 to 320 °C, the size and number of the clusters formed after the dehydration processes increase rapidly, then the clusters coalesce randomly and form small crystallites (weak Raman bands). These small crystallites grow into good quality

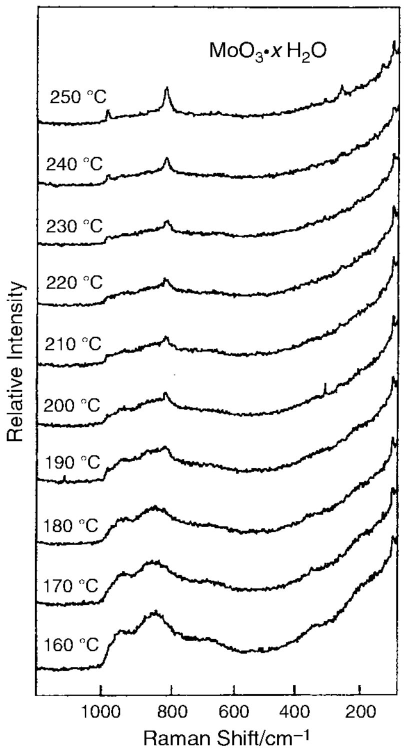

Fig. 4 Thermo-Raman spectra of as-synthesized hydrated MoO_3 in the vibration region of MoO_3 from 160 to 250 °C during dehydration.

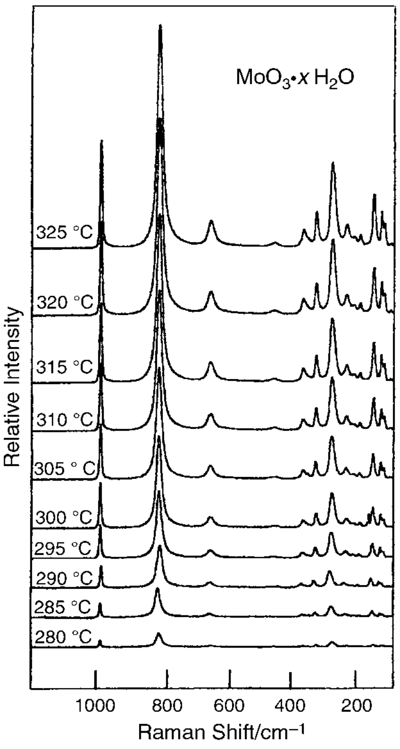

Fig. 5 Thermo-Raman spectra of as-synthesized hydrated MoO_3 in the vibration region of MoO_3 from 280 to 325 °C, suggesting possible formation of the MoO_3-II phase.

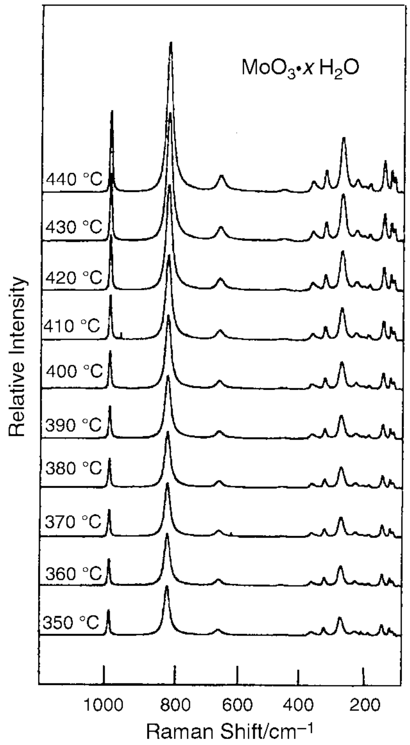

Fig. 6 Thermo-Raman spectra of as-synthesized hydrated MoO_3 in the vibration region of MoO_3 from 350 to 440 °C showing formation of the α-MoO_3 phase.

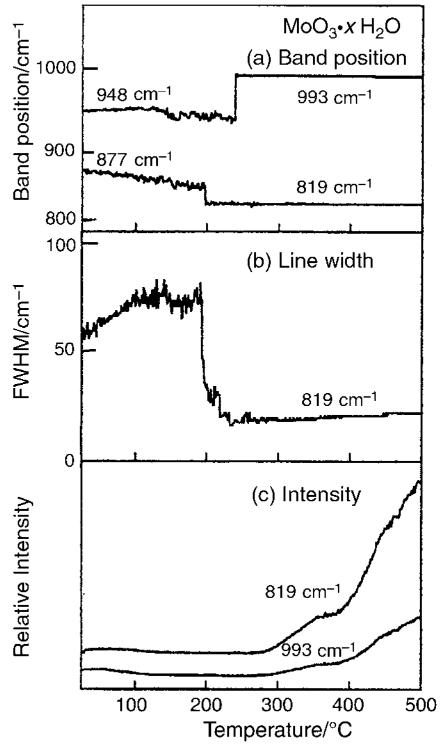

Fig. 7 Temperature dependence of (a) band positions of the dominant bands at 819 and 993 cm^{-1}, (b) line width of the band at 819 cm^{-1} and (c) intensities (area) of the dominant bands at 819 and 993 cm^{-1}.

crystals (strong Raman bands) of the MoO_3-II phase. The observation of an appreciable increase in the intensities of the terminal Mo–O stretching mode at 993 cm^{-1} and bridge Mo–O–Mo stretching mode at 819 cm^{-1} from 400 °C might be due to transformation of the MoO_3-II phase to α-MoO_3 phase. The spectrum observed at 440 °C was more similar to the α-MoO_3 phase spectrum at high temperature reported by earlier workers.[16]

Griffiths *et al.* revealed that the crystallization process would make the strong Raman bands in the amorphous phase narrower and shifted.[17] The evolution of the ν(Mo–O) mode at around 993 cm^{-1} and ν(Mo–O–Mo) mode around 819 cm^{-1} of the α-MoO_3 phase observed in this thermo-Raman process are shown in Fig. 7(a). The broad band observed at 877 cm^{-1}, due to as-synthesized hydrated MoO_3, gradually moves to lower wavenumber from120 to 197 °C, after the major dehydration process. It then shows a sharp shift to 819 cm^{-1}, indicating the formation of microcrystals, at 198 °C after the second dehydration process. There is some fluctuation in the position of this band up to 360 °C, but at higher temperatures it remains at 819 cm^{-1}. The sharp band observed at 948 cm^{-1} for as-synthesized hydrated MoO_3 shows no appreciable variation in its position up to 144 °C, then shifts gradually to lower wavenumber in the temperature interval 145 to 239 °C. The abrupt shift in its position to higher wavenumber, 993 cm^{-1}, at 240 °C signals the onset of crystallization after the third dehydration process and it remains at this position as the temperature increases further. The evolution of the strong crystalline band at 819 cm^{-1} from the band observed at 877 cm^{-1} for as-synthesized hydrated MoO_3, in terms of line width, (full width at half-maximum) is presented in Fig. 7(b) as a function of temperature. The line width of this band was around 59 cm^{-1} at 30 °C, increasing gradually to 83 cm^{-1} at 194 °C and becoming 25 cm^{-1} around 200 °C. Another drop in line width, to 20 cm^{-1}, was observed around 240 °C after the third dehydration process. The line width of this band showed minor fluctuations up to 360 °C then narrowed to 19 cm^{-1}. The investigation into the temperature evolution of these two strong bands revealed small shifts in their positions towards lower wavenumber during the major dehydration process and the appearance of crystalline bands at 819 and 993 cm^{-1} after the second and third dehydration processes, respectively.

Raman spectra are not only useful for identifying the phase, but can also show the evolution of the system from a disordered to a crystalline phase through changes in band intensities (area). Hence, in addition to the observation of spectral variation, a study of the intensities of the Raman bands would be useful to investigate the structural evolution from a disordered to a crystalline state. The intensities of the broad bands observed at 948 and at 877 cm^{-1} are presented in Fig. 7(c) as a function of temperature. The broad bands observed at 948 and 877 cm^{-1} due to as-synthesized hydrated MoO_3 show a slight drop in intensities in the temperature region 30 to 120 °C, corresponding to the dehydration process. After that, no change in their intensities was observed up to 289 °C, but from 290 to 355 °C the intensities of the crystalline bands at 993 and 819 cm^{-1} increase considerably, which indicates the transformation from amorphous to crystalline phase. An appreciable increase in their intensities observed from 400 °C indicates the transformation from the possible MoO_3-II phase to α-MoO_3.

Typical spectra in the thermo-Raman studies occur at (a) 30, (b) 125, (c) 220, (d) 255, (e) 280, (f) 350, (g) 420 °C and (h) room temperature after the heat treatment to 500 °C, as shown in Fig. 8A. They correspond to the characteristic spectra of (a) as-synthesized sample, (b) amorphous phase after the major weight loss, (c) amorphous phase after the second weight loss, (d) amorphous phase after the third weight loss, (e) onset of crystallization, (f) possible MoO_3-II phase, (g) α-MoO_3 phase at high temperature and (h) α-MoO_3 phase at room temperature, respectively.

The PXRD patterns of the as-synthesized hydrated MoO_3 sample and the samples after heat treatment to 125, 255, 310, 350, 420 and 500 °C are shown in Fig. 8B. The presence of two

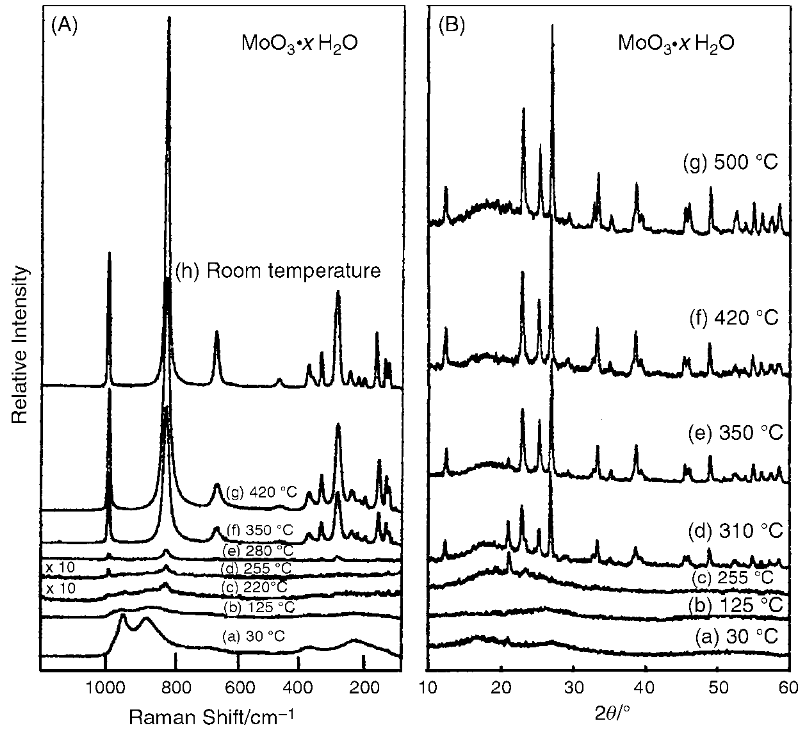

Fig. 8 A: typical thermo-Raman spectra of (a) as-synthesized hydrated MoO_3, (b) amorphous phase after the major weight loss, (c) amorphous phase after the second weight loss, (d) amorphous phase after the third weight loss, (e) onset of crystallization, (f) possible MoO_3-II phase, (g) α-MoO_3 phase at higher temperature and (h) α-MoO_3 phase at room temperature. B: PXRD patterns of (a) as-synthesized hydrated MoO_3 sample, sample after heat-treatment to (b) 125, (c) 255, (d) 310, (e) 350, (f) 420 and (h) 500 °C.

halos in the low angle region in the PXRD pattern of as-synthesized hydrated MoO_3 [Fig. 8B(a)] indicates the non-crystalline or highly disordered nature of the molecular arrangement. The presence of a broad weak peak from $2\theta = 21$ to 32° in the PXRD of the sample after heat treatment to 125 °C [Fig. 8B(b)] indicates the amorphous nature after the major dehydration process. The PXRD pattern for the sample after heat treatment to 255 °C, shown in Fig. 8B(c), displays two weak peaks at $2\theta = 21$ and 24° which indicates the onset of formation of sub-microcrystals in the amorphous matrix. The weak nature of the crystalline peaks and a halo in the low angle region of the PXRD pattern from the sample after heat treatment to 310 °C [Fig. 8B(d)] indicate the existence of a small amount of amorphous matrix with polycrystals. The increase in the intensity of the crystalline peaks in the PXRD pattern at 350 °C [Fig. 8B(e)] indicates an increase in the degree of crystallinity. The intensity of the peak observed at $2\theta = 21°$ decreases appreciably and the weak peak observed at $2\theta = 24°$ disappears completely in the PXRD corresponding to 350 °C. On further heat treatment, the PXRD showed an increase in the intensity of all the peaks except the peak at 21°, which disappears completely. The PXRD pattern for the sample after heat treatment to 500 °C agrees well with the reported α-MoO_3 phase structure. The presence of the two peaks around $2\theta = 21$ and 24° signals the slight difference in the crystalline structure at 310 °C compared to that after higher temperature treatment and also supports the existence of the possible MoO_3-II phase observed by thermo-Raman studies in that temperature interval.

$MoO_{3-\delta}$, with δ between 0.25 and 0.09, has been reported previously.[6] Spevack and McIntyre reported the reduction of MoO_3 to MoO_2 under flowing nitrogen and the presence of several intermediate oxides, and also indicated that the intermediate oxides are poor Raman scatterers and even Raman inactive.[18] Julien *et al.* reported the molybdic acid composed of $MoO_5 \cdot H_2O$ polyhedra and transformation to regular MoO_6 octahedra above 400 °C after completion of the dehydration processes.[19] Several authors have reported on the colors of various molybdenum oxides, molybdenum suboxides and their hydrated complexes and also changes in their color during the thermal process.[6,18,20] The light blue color of the as-synthesized hydrated MoO_3 sample indicates that the oxidation state of Mo was partially reduced. In order to understand the evolution of the as-synthesized hydrated MoO_3 sample in the thermal process from 25 to 500 °C at a heating rate of 5 °C min^{-1} under a flow of nitrogen gas, Raman spectra were collected continuously for every degree interval.

Typical thermo-Raman spectra observed under a flow of nitrogen gas are shown in Fig. 9(a) to (g). The thermo-Raman spectra shown in Fig. 9(a) to (d) are more or less similar to the spectra observed in air. In air, the spectra observed after the third weight loss around 240 °C clearly show an increase in intensity of the bands at 819 and 993 cm^{-1} and also the appearance of a few weak bands at lower frequencies which signal the formation of microcrystals. But under nitrogen, even the spectrum recorded at 400 °C did not show any appreciable increase in the intensity of the bands at 819 and 993 cm^{-1} or the bands at lower frequencies. However, when the sample was maintained at 400 °C and exposed to oxygen flow instead of nitrogen in the sample oven, within just 2 min the characteristic spectrum of crystalline α-MoO_3 appeared, as shown in Fig. 9(h). The above observation indicates that the sample formed after dehydration might be oxygen deficient $MoO_{3-\delta}$. The oxygen deficient $MoO_{3-\delta}$ destroys the translational symmetry of MoO_3 and, thus, leads to a change in the Raman scattering tensor. In air, the light blue as-synthesized sample changed to yellow around 400 °C. But under the nitrogen flow, it became dark purple at 400 °C and turned to yellow after exposure to an oxygen atmosphere. The different Raman scattering tensor of the oxygen deficient $MoO_{3-\delta}$ might be the reason for the difference in the spectral variations observed under nitrogen flow.

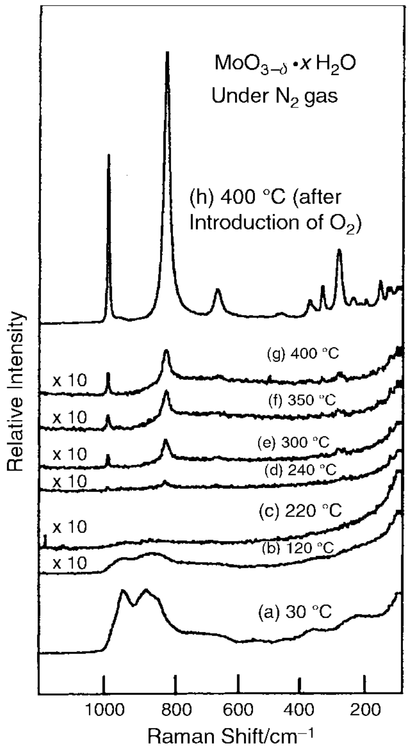

Fig. 9 Typical thermo-Raman spectra under nitrogen gas flow for (a) as-synthesized hydrated MoO_3 sample, (b) amorphous phase after the major weight loss, (c) amorphous phase after the second weight loss, (d) amorphous phase after the third weight loss, (e) at 300, (f) 350 and (g) 400 °C and (h) α-MoO_3 phase after the introduction of oxygen gas.

Conclusion

Thermally induced structural transformations in hydrated MoO_3 prepared by acidification of Na_2MoO_4 solution have been investigated dynamically by thermo-Raman spectroscopic techniques in this work. The spectral variation observed in the temperature interval 30 to 120 °C during the dynamic thermal process revealed the major dehydration process. The spectral variations observed in the temperature interval 160 to 240 °C indicated the effect of two more dehydration steps and the transformation to amorphous phase. The spectral variation observed in the temperature range 250 to 320 °C indicated the increase in size and number of clusters, formation of microcrystals and formation of possible MoO_3-II phase. The spectra in the temperature range 350 to 440 °C did not show any major change in the spectral profile but showed an appreciable enhancement in the intensities of the bands from 400 °C and the spectra were more similar to the reported α-MoO_3 phase spectrum. Investigations into the band positions, line widths (full width at half-maximum) and intensities of the dominant Raman bands as a function of temperature revealed the dehydration process, transformation from amorphous to crystalline phase and transformation from the possible MoO_3-II phase to α-MoO_3 phase. The thermal analysis and PXRD analysis carried out in this work provides strong support for all the results from the thermo-Raman studies. The structural evolution under a flow of nitrogen gas indicated that the sample formed after the dehydration processes could be oxygen deficient $MoO_{3-\delta}$. The different Raman scattering tensor of the oxygen deficient $MoO_{3-\delta}$ might be the reason for the difference in the spectral variations observed under nitrogen flow.

Acknowledgements

This work was supported by the National Science Council of the Republic of China (NSC-89-2113-M007-013 and NSC-88-CPC-M007-002).

References

1 F. A. Cotton and G. Wilkinson, *Advanced Inorganic Chemistry*, 4th edn., John Wiley, New York, 1980, p. 844.
2 L. Seguin, M. Figlarz, R. Cavagnat and J. C. Lassegues, *Spectrochim. Acta, Part A*, 1995, **51**, 1323.
3 G. Anderson and A. Magneli, *Acta Chem. Scand.*, 1950, **4**, 793.
4 E. M. McCarron III, *J. Chem. Soc., Chem. Commun.*, 1986, 336.
5 B. Baker, T. P. Feist and E. M. McCarron III, *J. Solid State Chem.*, 1995, **119**, 199.
6 E. Haro-Poniatowski, C. Julien, B. Pecquenard, J. Livage and M. A. Camacho-Lopez, *J. Mater. Res.*, 1998, **13**, 1033.
7 J. R. Gunter, *J. Solid State Chem.*, 1972, **5**, 354.
8 G. A. Nazri and C. Julien, *Solid State Ionics*, 1995, **80**, 271.
9 H. Chang and P. J. Huang, *Anal. Chem.*, 1997, **69**, 1485.
10 H. Chang and P. J. Huang, *J. Raman Spectrosc.*, 1998, **29**, 97.
11 R. Murugan, P. J. Huang, A. Ghule and H. Chang, *Thermochim. Acta*, 2000, **346**, 83.
12 R. Murugan, A. Ghule and H. Chang, *J. Appl. Phys.*, 1999, **86**, 6779.
13 R. Murugan, A. Ghule and H. Chang, *J. Phys.: Condens. Matter*, 2000, **12**, 677.
14 H. Chang, P. J. Huang and S. C. Hou, *Mater. Chem. Phys.*, 1999, **58**, 12.
15 M. A. Py and K. Maschke, *Physica B*, 1981, **105**, 370.
16 U. S. Ozkan, M. R. Smith and S. A. Driscoll, *J. Catal.*, 1992, **134**, 24.
17 J. E. Griffiths, G. P. Espinosa, J. P. Remika and J. C. Phillips, *Solid State Commun.*, 1981, **40**, 1077; J. E. Griffiths, G. P. Espinosa, J. P. Remika and J. C. Phillips, *Phys. Rev. B*, 1982, **25**, 1272.
18 P. A. Spevack and N. S. McIntyre, *J. Phys. Chem.*, 1992, **96**, 9029.
19 C. Julien, B. Yebka and G. A. Nazri, *Mater. Sci. Eng. B*, 1996, **38**, 65.
20 Y. Muraoka, J. C. Grenier, S. Petit and M. Pouchard, *Solid State Sci.*, 1999, 133.